WIND ENERGY
Wind Energ. 2006; **9**:39–53
Published online 11 January 2006 in Wiley Interscience
(www.interscience.wiley.com) **DOI**: 10.1002/we.189

Research Article

Analytical Modelling of Wind Speed Deficit in Large Offshore Wind Farms

Sten Frandsen*, Rebecca Barthelmie, Sara Pryor, Ole Rathmann, Søren Larsen and Jørgen Højstrup, Risø National Laboratory, DK-4000 Roskilde, Denmark
Morten Thøgersen, EMD, Aalborg, Denmark

Key words:
wind farm;
large;
efficiency;
analytical; model

The proposed model for the wind speed deficit in wind farms is analytical and encompasses both small wind farms and wind farms extending over large areas. As is often the need for offshore wind farms, the model handles a regular array geometry with straight rows of wind turbines and equidistant spacing between units in each row and equidistant spacing between rows. Firstly, the case with the flow direction being parallel to rows in a rectangular geometry is considered by defining three flow regimes. Secondly, when the flow is not in line with the main rows, solutions are suggested for the patterns of wind turbine units corresponding to each wind direction. The presentation is an outline of a model complex that will be adjusted and calibrated with measurements in the near future. Copyright © 2006 John Wiley & Sons, Ltd.

Received 22 November 2004; Revised 8 November 2005; Accepted 10 November 2005

Introduction

The engineering models presently applied for calculating production losses due to wake effects from neighbouring wind turbines are based on local 'unit-by-unit' momentum equations, disregarding the two-way interaction with the atmosphere. Other models, which did not reach engineering relevance or maturity, predict the array efficiency of infinitely large wind farms by viewing the wind turbines as roughness elements. A third option is to apply CFD schemes, which presently lack details and are computationally uneconomic.

The following presentation is an outline of a model complex that links the small-scale and large scale features of the flow in wind farms. Thus, if successful, it will be applicable for any size of wind farm. The model will be evaluated and adjusted and calibrated with measurements in the near future.

As is often the need for offshore wind farms, the model handles *a priori* a regular array geometry with straight rows of wind turbines and equidistant spacing between units in each row and equidistant spacing between rows. Firstly, the case with the flow direction being parallel to rows in a rectangular geometry is considered by defining three flow regimes. Secondly, when the flow is not in line with the main rows, solutions may be found for the patterns of wind turbine units emerging corresponding to each wind direction.

Counting from the upwind end of the wind farm, the model encompasses three regimes as illustrated in Figure 1. In the first regime the wind turbines are exposed to multiple-wake flow and an analytical link between the expansion of the multiple wake and the asymptotic flow speed deficit is derived. The second regime materializes when the (multiple) wakes from neighbouring rows merge and the wakes can only expand vertically

*Correspondence to: S. Frandsen, Risø National Laboratory, DK-4000 Roskilde, Denmark.
E-mail: sten.frandsen@risoe.dk
Contract/grant sponsor: Danish Public Service Obligation (PSO)

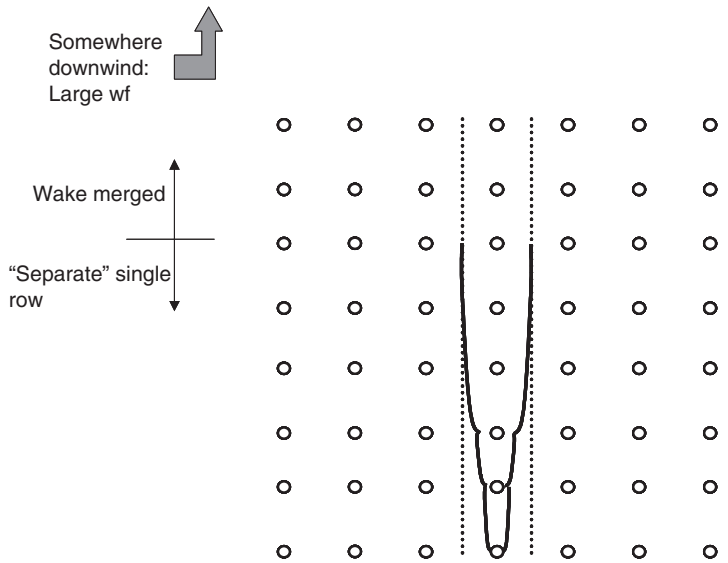

Figure 1. Illustration of the regimes of the proposed model. The wind comes from the 'south', parallel to the direction of the rows

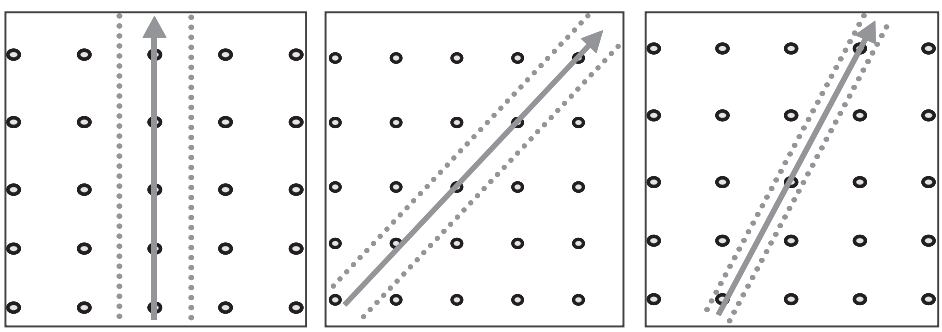

Figure 2. Examples of wind turbine patterns for different wind directions

upward. This regime corresponds (but is not identical) to the flow after a simple roughness change of terrain. The third regime is when the wind farm is 'infinitely' large and the flow is in balance with the boundary layer.

More regimes may need to be defined when the model is to be applied for practical solution. For example, the first row facing the wind is obviously not exposed to wake conditions and the wake hits the ground before it merges with the wakes from neighbouring rows. However, it is chosen to disregard these additional regimes in order to produce a clearer presentation.

Other wind directions are treated similarly. When the flow direction is not in line with the main rows, solutions are found for the patterns of wind turbine units emerging corresponding to each wind direction (Figure 2). The solutions are in principle the same as for the base case, but with different spacing in the along-wind direction and different distance to the neighbouring rows.

The regimes outlined above are discussed in detail in the following, and component models are described.

Single Wake

Initially the flow through and around the wind turbine rotor is considered. Lanchester[1] and Betz[2] derived expressions that link thrust and power coefficients of the wind turbine to the flow speed deficit of its wake. The main device for these derivations was a control volume with no flow across the cylinder surface.

DOI: 10.1002/we

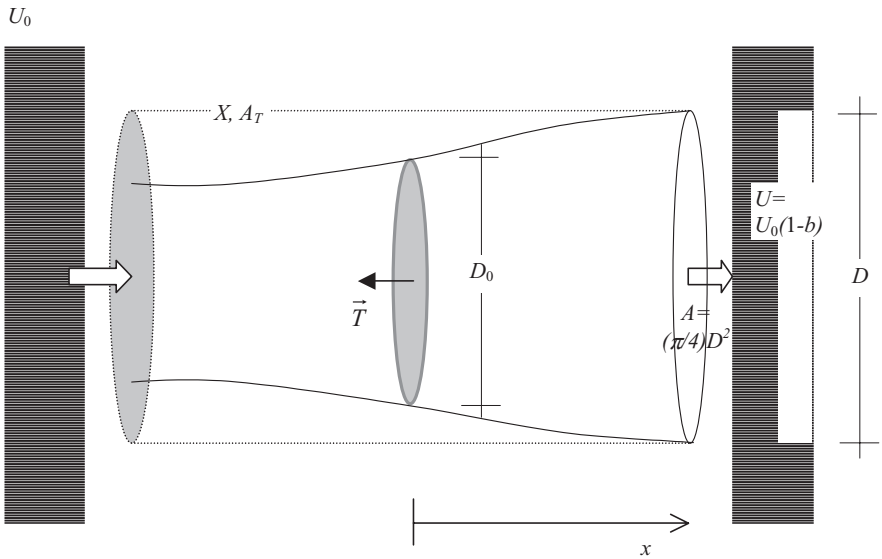

Figure 3. Control volume around a wind turbine rotor. The cylindrical control volume has the surface area A_T and volume X. The Betz control volume (full line) follows the streamlines

Alternatively—and this is practical in the present context—a cylindrical control volume with constant cross-sectional area equal to the wake area and with horizontal axis parallel to the mean wind vector is defined (Figure 3). From Reference 3 the momentum equation in vector form for the flow volume X with the surface area A_T is

$$\int_X \rho \frac{\partial \vec{U}}{\partial t} \mathrm{d}X + \int_{A_T} \rho \vec{U}\left(\vec{U}\mathrm{d}\vec{A}\right) = -\int_{A_T} p\mathrm{d}\vec{A} + \int_X \rho \vec{g}\mathrm{d}X + \vec{T} + \int_{A_T} \vec{\tau}\mathrm{d}A \tag{1}$$

where the acceleration term (first on the left-hand side), the pressure term (first on the right-hand side) and the gravity term (second on the right-hand side) often, as is done in the following, are neglected in basic considerations. Further, the cylinder extends upwind and downwind far enough* for the pressure to become equal to the freestream pressure. $\vec{T}$ is the sum of forces from obstacles acting on the interior of the control volume, and the last term on the right-hand side represents the turbulent shear forces acting on the control volume surface.

If it is acceptable to neglect shear forces in the cylinder surface and assume that pressure downwind has regained the freestream level, equation (1) conveniently reduces to

$$T = \int_A \rho U(U_0 - U)\mathrm{d}A \tag{2}$$

where A is the wake cross-sectional area, which may be definite or infinite, and U_0 and U are the free and wake flow wind speeds respectively. A possible rotation of the flow generated by the propeller has been neglected. This expression is a classical starting point for development of wake models (see e.g. References 3–5). The next step in evaluation of the wake characteristics is to assume self-similarity of the wake flow speed profiles, i.e. the wake wind profile can be written as

$$U = U_\mathrm{w}(x) f(r/R) \tag{3}$$

where U_w is the minimum wake flow speed, r is the distance from the centre of the wake and R is a characteristic of the wake width at the distance x downwind of the rotor. Assuming that the wake is axisymmetric, inserting equation (3) into (2) and introducing polar co-ordinates and the substitution $y = r/R$ yields

*Upstream of the order 0·5–1 rotor diameter and downwind 2–3 rotor diameters.

DOI: 10.1002/we

$$T = \int_0^{2\pi}\int_0^{\infty} \rho r U_w f(r/R)(U_0 - U_w) f(r/R)\mathrm{d}r \quad \Rightarrow \quad T \propto \rho R^2 \int_0^{\infty} y U_w f(y)(U_0 - U_w f(y))\mathrm{d}y \tag{4}$$

The integral in (4) depends only on the minimum wake flow speed U_w. Therefore equation (4) can be written as

$$T = C_{f1}\rho\pi R^2 U_w'(U_0 - U_w') \tag{5}$$

where $U_w' = C_{f2}U_w$ is a characteristic flow speed and C_{f1} and C_{f2} are constants depending only on the integrals $\int_0^{\infty} f(y)\mathrm{d}y$ and $\int_0^{\infty} f^2(y)\mathrm{d}y$ respectively, i.e. the *shape* of the wake profile. The assumption of self-similarity throughout the wake is not only questionable in general terms for the regions of the wake, which is of interest in the present context, it is definitely wrong in the near-wake region. However, the self-similarity assumption maintained here is justified because the wake-affected wind turbine's rotor 'integrates' the wake over a sizable fraction of its area, thus making the finer details less important.

Thus any actual wake shape can be represented by a rectangular distribution of the flow speed without violating the general principles of the above derivations:

$$T = \rho A U(U_0 - U), \qquad A = \frac{\pi}{4} D^2 \tag{6}$$

where D is the diameter of the rectangular wake flow speed profile and A is the area of the wake. In (6), U is a function of x but not of r. The thrust may also be expressed as

$$T = \tfrac{1}{2}\rho A_0 U_0^2 C_T \qquad A_0 = \tfrac{\pi}{4} D_0^2 \tag{7}$$

where A_0 is the swept area of the rotor, D_0 is the rotor diameter and C_T is the thrust coefficient. As pointed out previously, the derived expression is only valid some distance downwind of the rotor where the pressure has regained its free flow value. Denoting the induction factor* as $a = 1 - U_a/U_0$, where U_a is the flow speed in the wake just after the initial wake expansion, then the thrust coefficient is related to the induction factor by

$$C_T = a(2 - a) \quad \Rightarrow \quad a = 1 - \sqrt{1 - C_T}, \quad C_T < 1 \tag{8}$$

and the wake cross-sectional area immediately after wake expansion, A_a, is related to the rotor area by

$$\frac{A_a}{A_0} = \frac{1 - a/2}{1 - a} \tag{9}$$

Combining equations (6)–(9) yields

$$A_a = \beta A_0 \text{ and } D_a = \sqrt{\beta} D_0, \text{ where } \beta = \frac{1}{2}\frac{1 + \sqrt{1 - C_T}}{\sqrt{1 - C_T}} \tag{10}$$

As indicated previously, the result applies to the wake area at the position downwind where the pressure in the wake has regained the free flow value. In real terms it is difficult to identify exactly that position. Here we choose to assume that the wake expands immediately. Thus, denoting the wake area at distance x downwind from the wind turbine as $A = A(x)$, the assumption is that $A(x = 0) = A_a$. The assumption is crude but ensures a solution for all C_T values between 0 and 1 of the combined equations (6) and (7) (see later).

The following expression for the wake flow speed is found:

$$\frac{U}{U_0} = \frac{1}{2} \pm \frac{1}{2}\sqrt{1 - 2\frac{A_0}{A} C_T} \tag{11}$$

*Usually the induction factor is defined through the flow speed in the rotor plane.

DOI: 10.1002/we

For $A(x = 0) = A_a$, equation (11) has solutions for $0 \le a \le 1$, where the '+' applies for $a \le 0{\cdot}5$ and the '−' for $a > 0{\cdot}5$. Assuming monotonic expansion of the wake for increasing x, equation (11) only has solutions for $a \le 0{\cdot}5$. A frequently applied approximation to (6) for small wake flow speed deficits is $T \approx \rho A U_0(U_0 - U)$, which in turn modifies equation (11):

$$\frac{U}{U_0} \approx 1 - \frac{1}{2} C_T \frac{A_0}{A} \approx 1 - a\frac{A_0}{A} \tag{12}$$

In principle this equation has solutions for all distances downwind and for all $0 \le a \le 1$. The above considerations only allow direct estimation of the *initial* wake flow speed deficit. In order to estimate the deficit any distance downwind, a model for the wake expansion must be identified.

Schlichting,[4] Engelund[3] and others point to a solution where $D \propto x^{1/3} \Rightarrow A \propto x^{2/3}$ for $x \sim \infty$.

The result stems from several assumptions (most prominent are constant eddy viscosity in the wake and self-similarity of the wake flow speed deficit and turbulence profiles) and is only valid in the far wake where the approximation of (12) in practical terms is also valid. Therefore it is useful to adopt a model for expansion of the wake cross-sectional area as a function of distance downwind that has the form

$$D(x) = \left(\beta^{k/2} + \alpha s\right)^{1/k} D_0, \qquad s = x/D_0 \tag{13}$$

where the initial wake diameter is $\sqrt{\beta} D_0$. If the Schlichting solution is chosen, then $k = 3$. The constant α must be determined experimentally. An initial estimate could be obtained by comparing equation (13) with a model developed by Jensen[6] and further by Katic *et al.*:[7]

$$D_{(\mathrm{noj})}(x) = (1 + 2\alpha_{(\mathrm{noj})} s) D_0, \qquad \frac{U}{U_0} = 1 - a\frac{A_0}{A_{(\mathrm{noj})}} = 1 - a\frac{D_0^2}{D_{(\mathrm{noj})}^2} \tag{14}$$

where $\alpha_{(\mathrm{noj})} \approx 0{\cdot}05$. In this model the initial expansion of the wake has been neglected and the linear wake expansion is presumably too large. However, applied in the wind resource computer code WAsP,[8] the model has proven successful for wind farms of limited size. Matching the expressions (13) and (14) for wake flow speeds at distance s downwind yields

$$\left(\beta^{k/2} + \alpha s\right)^{2/k} = \beta(1 + 2\alpha_{(\mathrm{noj})} s)^2 \quad \Rightarrow \quad \alpha = \beta^{k/2}\left[(1 + 2\alpha_{(\mathrm{noj})} s)^k - 1\right] s^{-1} \tag{15}$$

Figure 4 shows the relative wake wind speed as function of downwind distance from the wake-generating wind turbine for different wake shapes and with and without the linearization of (11). Obviously, the decay factor depends on the distance downwind chosen to match the flow speeds. For small C_T and large s the decay factor α is of order $10\alpha_{(\mathrm{noj})}$. The square root shape ($k = 2$) is chosen for reasons given hereafter.

Multiple Wake, Single Row (Regime 1)

The case of multiple wakes is dealt with as illustrated in Figure 5. Firstly, the possible effects from boundaries such as the ground are included implicitly through the area growth $\mathrm{d}A_n = A_{n+1} - A_n$. We consider a single row of wind turbines and in that row the wake between wind turbine n and wake $n + 1$ is described. Outside the cylinder surface of the control volume the flow speed is U_0. The wake flow speed is assumed constant. The flow speed at the ends of the cylinder surface is denoted as indicated in Figure 5. The areas corresponding to the diameters D_n are denoted A_n and now refer to a position just in front of each unit. Note also that the cross-section of the control volume need not be a circular cylinder.

Without the approximation of (12), we get for momentum conservation

DOI: 10.1002/we

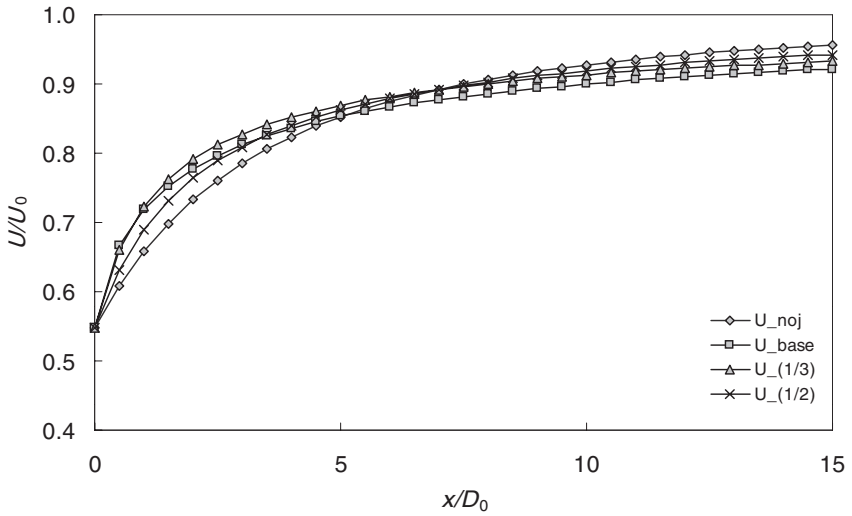

Figure 4. Comparison of single-wake models: 'U_(1/2)' is the proposed model, 'U_(1/3)' is the Schlichting[4] model, 'U_noj' is the Jensen[6] model and 'U_base' is the Schlichting model with no linearization of the momentum equation. The figure gives the relative speed in the wake as a function of downwind position. $C_T = 0{\cdot}7$, $2\alpha_{(noj)} = 0{\cdot}1$; the flow speed deficits were matched at $s = x/D_0 = 7$

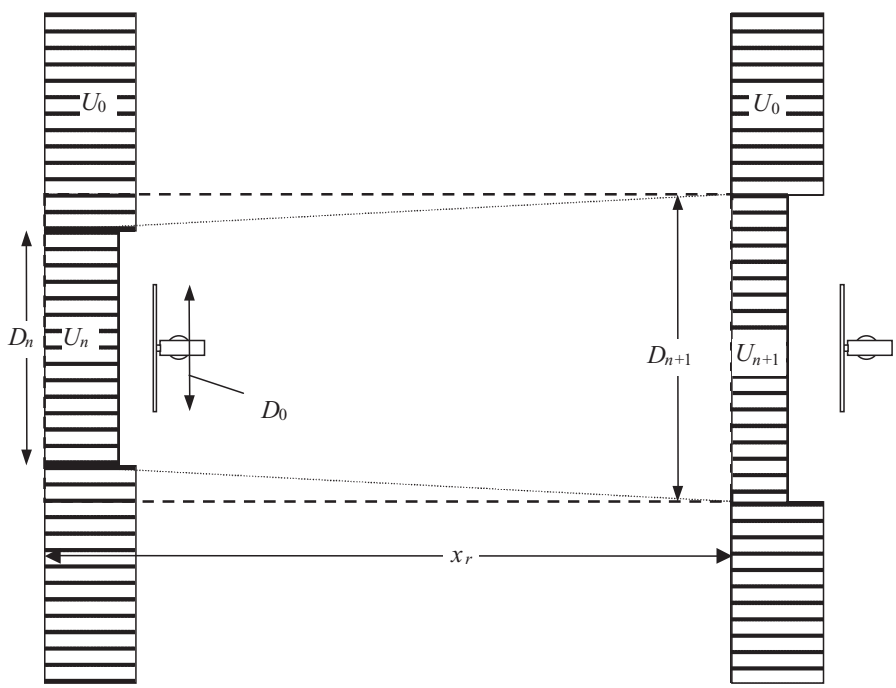

Figure 5. Flow between two units in a long row of wind turbines

DOI: 10.1002/we

$$\rho A_{n+1}U_{n+1}(U_0 - U_{n+1}) = \rho(A_{n+1} - A_n)U_0(U_0 - U_0) + \rho A_n U_n(U_0 - U_n) + T \quad \Rightarrow$$
$$A_{n+1}U_{n+1}(U_0 - U_{n+1}) = A_n U_n(U_0 - U_n) + \frac{1}{2}A_R U_n^2 C_T \quad \Rightarrow$$
$$c_{n+1}(1 - c_{n+1}) = \frac{A_n}{A_{n+1}}c_n(1 - c_n) + \frac{1}{2}\frac{A_R}{A_{n+1}}c_n^2 C_T, \qquad c_n = \frac{U_n}{U_0}, \qquad c_{n+1} = \frac{U_{n+1}}{U_0} \tag{16}$$

where

$$A_n = A_n(s) = A_n(ns_r), \qquad s_r = x_r/D_0$$

is a function of the dimensionless distance s from the first wind turbine. *With* the approximation of the flow speed deficit, equation (12), the recursive equation becomes

$$c_{n+1} = 1 - \left(\frac{A_n}{A_{n+1}}(1 - c_n) + \frac{1}{2}\cdot\frac{A_R}{A_{n+1}}C_T c_n\right) \tag{17}$$

For a solution, an explicit model for the wake expansion is needed.

Asymptotically for n → ∞

For an infinitely large number of wind turbines it must be assumed that there is an asymptotic, non-zero wake flow speed. If the flow speed becomes zero, then the thrust on the wind turbines becomes zero and the flow will accelerate, etc. Therefore, for $n \to \infty$, $(c_n - c_{n+1}) \to 0$. Denoting the asymptotic value of the ratio as $c_w = c_n|_{n\to\infty}$ for large n, an equation linking the asymptotic wake area and wake flow speed is obtained:

$$c_w(1 - c_w) = \frac{A_n}{A_{n+1}}c_w(1 - c_w) + \frac{1}{2}\frac{A_R}{A_{n+1}}c_w^2 C_T \quad \Rightarrow \quad A_{n+1} - A_n = \frac{1}{2}A_R\frac{c_w}{1 - c_w}C_T \tag{18}$$

In (18), the term

$$\frac{1}{2}A_R\frac{c_w}{1 - c_w}C_T$$

is a constant and thus, asymptotically, the wake cross-sectional area is expanding linearly with x. Equation (18) points to an interesting result. With less than conventional assumptions it is possible to derive the wake expansion for an infinite row of two-dimensional obstacles: $D \propto x^{1/2}$. This expansion is the only shape that asymptotically will ensure a non-vanishing and non-increasing flow speed.

By assuming the wake cross-section to be circular, it is now possible to link the decay factor α in (15) to the asymptotic flow speed ratio c_w for the case of an infinite row of wind turbines. With the wake model of (15) with $n = 2$ corresponding to the square root expansion of wake diameter, the increase in wake cross-section is

$$A_{n+1} - A_n = \frac{\pi}{4}D_0^2[\beta + \alpha s_r(n+1)] - \frac{\pi}{4}D_0^2(\beta + \alpha s_r n) = A_R\alpha s_r \tag{19}$$

where s_r is the dimensionless distance between the wind turbines in the row. Inserting equation (19) into (18) yields

$$\alpha = \frac{1}{2}\frac{C_T}{s_r}\frac{c_w}{1 - c_w} \tag{20}$$

DOI: 10.1002/we

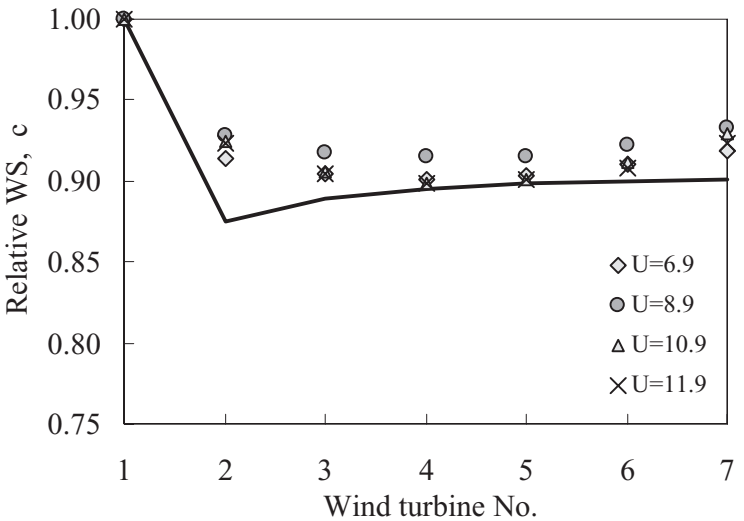

Figure 6. Measurement of wind speed ratio c_i at Nørrekær Enge II. Wind speeds are derived from power signals. Average is taken over six rows, each with seven units. $s_r \approx 7$. The wind farm consists of 42,300 kW units

Thus, if the asymptotic, relative flow speed in the wake is known from e.g. measurements, then the decay constant is given. Conversely, the relative wake flow speed c_w is given as

$$c_w = \frac{\alpha}{\alpha + \frac{1}{2} C_T / s_r} \tag{21}$$

In Figure 6 the result of applying equation (19) to data from the wind farm Nørrekær Enge II is shown. It is seen that the flow speed ratio is only marginally dependent on the free flow mean wind speed, i.e. c_w is approximately constant. With a C_T measured on a wind turbine similar to the units in question[9] and with these measurements approximated by $C_T \approx 3{\cdot}5(2U - 3{\cdot}5)U^{-2}$, it is found that the decay constant must be proportional to C_T to satisfy equation (20). The full line in Figure 6 is the model result, applying the average value of C_T for the four different wind speeds.

The consequence of a flow speed ratio c_w not being dependent on wind speed is that the decay constant α is a function of C_T, i.e. the initial wake deficit/turbulence.

Multiple Wake, Merged (Regime 2)

When the wakes from neighbouring rows meet, the wake expansion in lateral directions stops and the wake can only expand upward. Since the area must, asymptotically, expand linearly to satisfy equation (18), the height of the wake must increase linearly. This implies that the growth of what is equivalent to the internal boundary layer for roughness change models asymptotically has $h \propto x$.

Since the wake cannot expand laterally, the incremental growth of the internal boundary layer in regime 2 in the limit for $n \to \infty$ is

$$\Delta h = \frac{dA}{s_r D_0} = \frac{A_{n+1} - A_n}{s_r D_0} \tag{22}$$

and

DOI: 10.1002/we

$$\frac{\partial h}{\partial x} \approx \frac{A_{n+1}-A_n}{\Delta x}\frac{1}{s_r D_0} = \frac{1}{2}A_R \frac{c_{mw}}{1-c_{mw}} C_T \frac{1}{\Delta x}\frac{1}{s_r D_0} = \frac{1}{2}\frac{c_{mw}}{1-c_{mw}}\frac{\pi}{4} D_0^2 C_T \frac{1}{s_f D_0}\frac{1}{s_r D_0} \quad \Rightarrow$$

$$\frac{\partial h}{\partial x} \approx \frac{c_{mw}}{1-c_{mw}} c_t \quad \Rightarrow \quad h = \frac{c_{mw}}{1-c_{mw}} c_t (x - x_0) + h_0, \qquad c_t = \frac{\pi C_T}{8 s_r s_f} \tag{23}$$

where s_f is the dimensionless distance to the neighbouring rows, c_{mw} is the relative flow speed in the wake and x_0 and h_0 are integration constants to be determined. We want to make a comparison of this result with that of Elliott,[10] who suggested the following expression for the growth of an internal boundary layer after a change in terrain roughness:

$$h \approx 0{\cdot}8 x^{4/5} z_{00\infty}^{1/5}$$

where $z_{00\infty}$ is the roughness after this roughness change. For this purpose we choose the following values of the parameters:

$$s_r = s_f = 7, \qquad C_T = 0{\cdot}5, \qquad D_R = h_H = 100\text{m}$$

where h_H is the hub height. Assuming—as a little less than arbitrary—that the asymptotic wind speed is identical to the flow speed for the infinitely large wind farm, it is found that

$$z_{00} = 0{\cdot}55m, \qquad \frac{\partial h}{\partial x} = 0{\cdot}019$$

where z_{00} is the apparent roughness for the infinitely large wind farm (see later). Further, assuming that in regime 1 the wake expands similarly in lateral and vertical directions from hub height, we estimate the height of the multiple wakes when these merge with neighbouring rows as

$$h_0 \approx h_H + \frac{1}{2} s_f D_R \approx 5 D_R \approx 500\text{m}$$

(with better experimental information the suggested wake expansion model should be used). The distance downwind from the edge of the wind farm to where the wakes merge is here estimated as

$$x_0 \approx 10 h_0 = 5000\text{m}$$

In Figure 7 the growth of the internal boundary layer is plotted for Elliott's model and for the proposed model with the above tentative parameter values. As to the functional dependence on distance downwind, the

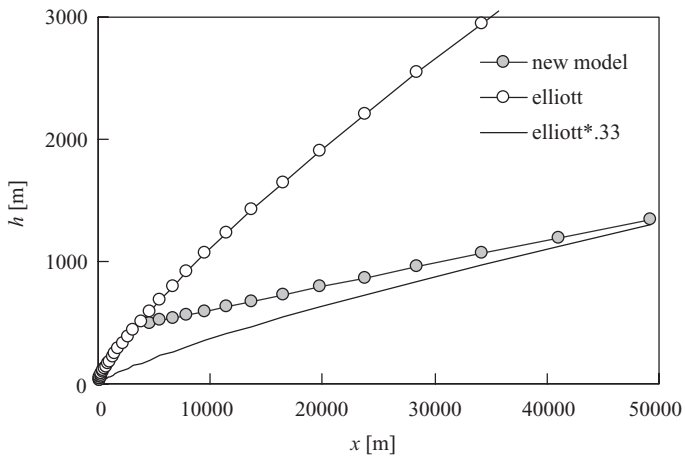

Figure 7. Growth of internal boundary layer as a function of downwind distance to front end edge of wind farm

DOI: 10.1002/we

model compares well with the Elliott model. The Elliott model estimates the internal boundary approximately three times higher than the proposed model. However, Sempreviva *et al.*[11] suggest that Elliott's result for h should be multiplied by 0·3 to fit experimental evidence, and with that modification to Elliott's model the agreement is good.

Wind Farm in Balance with Boundary Layer (Regime 3)

A model for the effect of a very large wind farm on the planetary boundary layer (PBL)[12–14] is outlined in the following. The first similar approach to the problem was given by Templin[15] and Newman,[16] who, together with a few others,[17] pioneered the discipline. At the time the approach was considered far-fetched by most people, since wind farms extending many kilometres seemed totally unrealistic. The model presented below refines that of Newman[16] and links the surface wind to the geostrophic wind speed by defining two flow layers divided at the wind turbine hub height and by introducing the geostrophic drag law.

The geostrophic drag law is derived by assuming that the inertial and viscous forces are small (low Rossby and Ekman numbers) relative to the Coriolis and friction forces respectively and the pressure force. The drag law for neutral atmospheric stratification can be written as[5]

$$G = \frac{u_*}{\kappa}\sqrt{\left[\ln\left(\frac{u_*}{fz_0}\right) - A\right]^2 + B^2} \tag{24}$$

Here μ_* is the friction velocity, z_0 is the surface roughness, $f = 2\Omega\sin\phi$ is the Coriolis parameter and G is the geostrophic wind speed. Ω is the angular speed of the Earth and ϕ is the latitude. A and B are constants, estimated by Troen and Petersen[8] to be $A = 1{\cdot}8$ and $B = 4{\cdot}5$.

Equation (28) is implicit in u_* and for practical purposes an approximation is useful. Jensen[18] proposed such an approximation, and with an adjustment to that approximation proposed by Emeis and Frandsen,[13] the geostrophic drag law becomes

$$G \approx \frac{u_*}{\kappa}\left[\ln\left(\frac{G}{fz_0}\right) - A_*\right] \quad \Leftrightarrow \quad u_* \approx \frac{\kappa G}{\ln\left(\frac{G}{fz_0}\right) - A_*} = \frac{\kappa G}{\ln\left(\frac{G}{\left(f\cdot \mathrm{e}^{A_*}\right)z_0}\right)} \tag{25}$$

where the constant by comparison with (24) is estimated to be $A_* \approx 4$ at latitude 55°.

Returning to the model for the influence of the wind farm on the local wind climate (see Figure 8), the following assumptions are made.

- The wind farm is large enough for the horizontally averaged, vertical wind profile to be horizontally homogeneous.
- The thrust on the wind turbine rotors is assumed to be concentrated at hub height.
- The horizontally averaged vertical wind profile is logarithmic over hub height and logarithmic under hub height. This assumption is similar to the assumption for the development of the internal boundary layer after a change of surface roughness.
- The vertical wind profile is continuous at hub height.
- Horizontally averaged turbulent wind speed fluctuations are horizontally homogeneous.
- The height of the PBL is considerably larger than wind turbine hub height: $H >> h_H$. Here we could comment that, forced by technology, this assumption is now only partly satisfied, depending on which boundary layer height is chosen.

Given that the last assumption is violated, this will be addressed further in later versions of the model.

The model for an infinitely large wind farm has been reported previously.[12,14] The apparent 'wind farm roughness' z_{00} may be expressed as

DOI: 10.1002/we

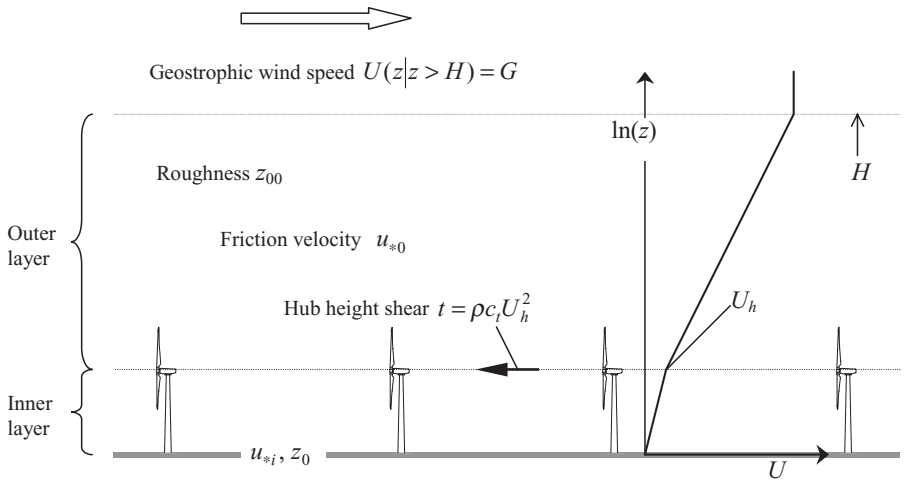

Figure 8. The impact of an 'infinitely' large wind farm on the planetary boundary layer. The difference between G and U_h is exaggerated

$$z_{00} = h_H \exp\left(-\frac{\kappa}{\sqrt{c_t + \left[\kappa / \ln(h_H / z_0)\right]^2}} \right) \tag{26}$$

In particular, for close spacing of the wind turbines, i.e. large wind speed deficits, this model results in significantly less wind speed deficit than Newman's model. In the absence of experimental evidence for infinitely large wind farms, the model will provide the asymptotic hub height flow speed ratio c_{wf}, for an increasing depth of the wind farm in regime 2.

Other Wind Directions

In the regular wind turbine array, other wind directions, are to be treated similarly. For each wind direction, new rows (with larger wind turbine spacing) will form, with new (smaller) distances between rows (see Figure 2). The *general* applicability of the proposed model will depend on whether the model—once calibrated by means of measurements—works for all wind directions.

Summary

Summarizing, the model has the following components.

1. From wake 2 or 3 to where the wake merges with neighbour-row wakes, use 'row of wind turbines' wake shape expanding in two directions:

$$\frac{D_R}{D} = \frac{1}{(\beta + \alpha \cdot s_r)^{1/2}}$$

The asymptotic relative wake speed deficit $c = U/U_0$ has—if the row is long enough—an asymptotic value c_1. The specific value is found from experiments and this value determines the decay constant α.

2. From the point of neighbour-wake merging and onward, the merged wake expands linearly upward:

$$h = \frac{c_{mw}}{1 - c_{mw}} c_t (x - x_0) + h_0$$

DOI: 10.1002/we

where x_0 and h_0 in principle are derived from the characteristics of the flow exiting regime 1.

3. Determine the relative flow speed deficit for the model from the infinitely large wind farm, c_{wf}. The first approximation is that $c_{mw} = c_{wf}$.

Apart from determining the efficiency of the wind farm, the estimation of the growth of the internal boundary layer is needed to determine what happens downwind.

The Appendix provides further details on the steps taken to operationalize the model.

Conclusion

Present-day and near-future offshore wind farms extend 5–10 km, which in relation to the boundary layer is 'large' but not 'infinitely' large. Thus there is a need for a model that handles both single and multiple wakes *and* the wind farm's interaction with the atmospheric boundary layer.

It is believed that the suggested model will—with appropriate experimental calibration—encompass the flow characteristics of very large wind farms in a realistic and consistent manner.

The model will be verified/calibrated by means of existing data and data from the large offshore demonstration projects at Horns Rev and Nysted.

To verify experimentally the flow speed deficit in the infinitely large wind farm, c_{wf}, will be difficult and is presently viewed as a major challenge.

Experimental data[19] show significant speed-up of the flow in between the rows, indicating that the flow is constrained already before the wakes from neighbouring rows merge in the sense described above. It is believed that the proposed model can handle this by appropriate adjustments.

Currently the model only allows simple geometries and there is a need to extend it to irregular geometries.

Acknowledgement

The work has been financed in part by Danish Public Service Obligation (PSO) funds.

Appendix: Implementation

The model has been operationalized ensuring that momentum is conserved at each model step (currently 1 m distance) in the three regimes.

Regime 1. Axisymmetric Expansion

By utilizing the equations given above, the expansion of the wake is as a circular disc (= axisymmetric). The primary variable is the wake height. Once the wake radius (height) exceeds the hub height, the wake is considered to have impacted the ground surface. The total momentum deficit is conserved but the area of the wake is computed by removing the below-ground portion (Figure 9). This occurs at approximately 10 rotor diameters (D) distance downstream of the turbine.

Regime 2. Multiple Merged Wakes

In the second regime, neighbouring wakes merge. This occurs at ~30D when half the wake width equals the turbine spacing. Again the total momentum deficit is conserved. The area of wake expansion is calculated as the above ground area minus half the overlapping sector as shown in Figure 9.

The model has been implemented using the Bonus 500 kW wind turbine thrust curve,[9] with a hub height of 38 m and a rotor diameter of 35 m. In the case study shown in Figure 10, the freestream wind speed is

DOI: 10.1002/we

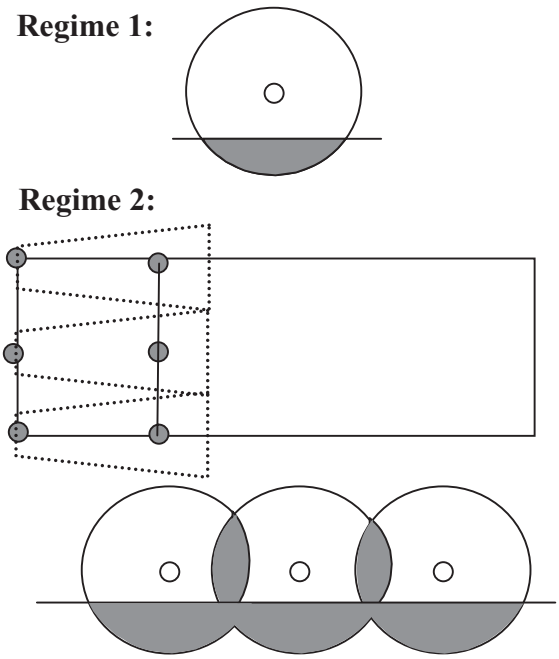

Figure 9. Illustration of the wake expansion model in regime 1, where the single wake expands and impacts the ground, and regime 2, where wakes merge with neighbouring wakes

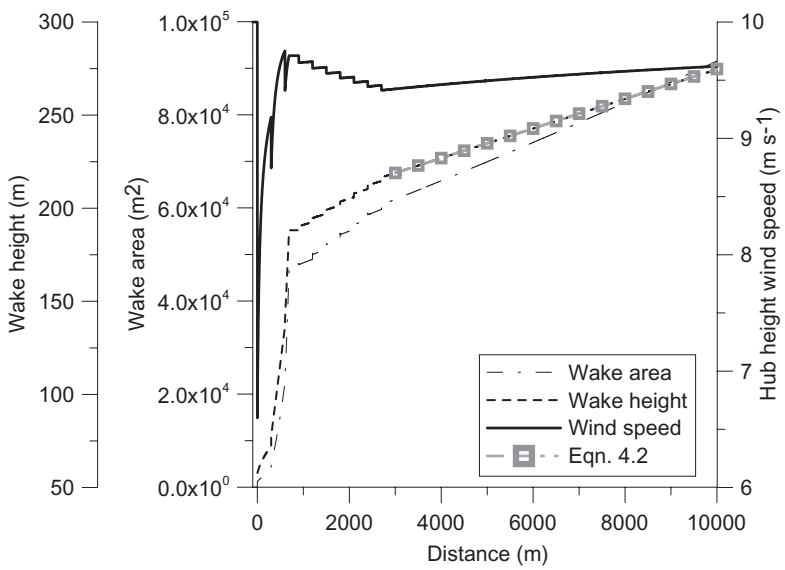

Figure 10. A model case study with a freestream wind speed of 10 m s^{-1} for a wind farm with 10 rows. The wake height, wake area and wind speed are shown for the turbine in the centre of the row

DOI: 10.1002/we

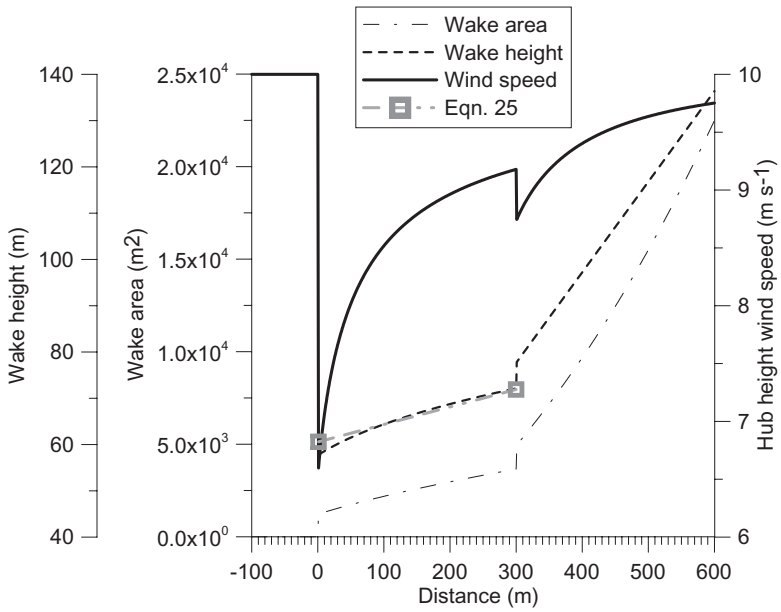

Figure 11. The model operationalized for a wind farm with 10 rows (for the first two rows). The wake height, wake area and wind speed are shown for the turbine in the centre of the row

10 m s^{-1} and the wind farm contains 10 rows, each of three turbines, with between- and along-row spacing of 300 m. Figure 10 shows the hub height wind speed passing through the wind farm (1–3000 m) and then for a further 7000 m.

Figure 11 shows a close-up of the first 600 m of the wind farm with two rows. The wake-height increases for the first wake, but then the two wakes merge giving a rapid increase in the wake area. As shown, the expansion of the single wake follows the single-wake shape equation. The double-wake expansion cannot be compared directly, because the total wake area for the wind farm is the area expanding in the model version. However, after the wind farm the development of the wake height follows the expansion given in 23 (see Figure 10).

References

1. Lanchester FW. Contribution to the theory of propulsion and the screw propeller. *Transactions of the Institution of Naval Architects* 1915; **LVII**: 98–116.
2. Betz A. Der Maximum der theoretisch mölichen Ausnützung des Windes durch Windmotoren. *Zeitschrift für das Gesamte Turbinenwesen* 1920; **26**: 307–309.
3. Engelund FA. *Hydraulics, the Mechanics of Newtonian Fluids*. Private Engineering Fund, Technical University of Denmark, 1968; 322 (in Danish).
4. Schlichting H. *Boundary Layer Theory* (6th edn). McGraw-Hill: New York, NY, 1968.
5. Tennekes H, Lumley JL. *A First Course in Turbulence*. MIT Press: Cambridge, MA, 1972.
6. Jensen NO. A note on wind turbine interaction. *Risø-M-2411*, Risø National Laboratory, Roskilde, 1983.
7. Katic I, Højstrup J, Jensen NO. A simple model for cluster efficiency. *Proceedings of European Wind Energy Conference and Exibition*, Rome, 1986; 407–410.
8. Troen I, Petersen EL. *European Wind Atlas*. Risø National Laboratory: Roskilde, 1989.
9. Frandsen S, Chacon L, Crespo A, Enevoldsen P, Gomez-Elvira R, Hernandez J, Højstrup J, Manuel F, Thomsen K, Sørensen P. Measurements on and modelling of offshore wind farms. *Risø-R-903(EN)*, Risø National Laboratory, Roskilde, 1996.
10. Elliott WP. The growth of the atmospheric internal boundary layer. *Transactions of the American Geophysical Union* 1958; **39**: 1048–1054.

DOI: 10.1002/we

11. Sempreviva AM, Larsen SE, Mortensen NG, Troen I. Response of neutral boundary layers to changes of roughness. *Boundary-Layer Meteorology* 1990; **50**; 205–225.
12. Frandsen S. On the wind speed reduction in the center of large clusters of wind turbines. *Journal of Wind Engineering and Industrial Aerodynamics* 1992; **39**: 251–265.
13. Emeis S, Frandsen S. Reduction of horizontal wind speed in a boundary layer with obstacles. *Boundary-Layer Meteorology* 1993; **64**: 297–305.
14. Frandsen S, Madsen PH. Spatially average of turbulence intensity inside large wind turbine arrays. *European Seminar on Offshore Wind Energy in the Mediterranean and Other European Seas (OWEMES 2003)*, Naples, 2003.
15. Templin RJ. An estimation of the interaction of windmills in widespread arrays. *Laboratory Report LTR-LA-171*, National Aeronautical Establishment, Ottawa, 1974.
16. Newman BG. The spacing of wind turbines in large arrays. *Journal of Energy Conversion* 1977; **16**: 169–171.
17. Bossanyi EA, Maclean C, Whittle GE, Dunn PD, Lipman NH, Musgrove PJ. The efficiency of wind turbine clusters, *Proceedings of Third International Symposium on Wind Energy Systems (BHRA)*, Copenhagen, 1980; 401–416.
18. Jensen NO. Change of surface roughness and the planetary boundary layer. *Quarterly Journal of the Royal Meteorological Society* 1978; **104**; 351–356.
19. Højstrup J, Courtney M, Christensen CJ, Sanderhoff P. Full-scale measurements in wind turbine arrays. Nørrekær Enge II. CEC/Joule. Risø report I684 1993.

DOI: 10.1002/we